

Effects of different friction stir welding conditions on the microstructure and mechanical properties of copper plates

Ali Alavi Nia and Ali Shirazi

Department of Mechanical Engineering, Bu-Ali Sina University, Hamedan, 651754161, Iran.
(Received: 15 November 2015; revised: 22 January 2016; accepted: 25 January 2016)

Abstract: Friction stir welding is a new and innovative welding method used to fuse materials. In this welding method, the heat generated by friction and plastic flow causes significant changes in the microstructure of the material, which leads to local changes in the mechanical properties of the weld. In this study, the effects of various welding parameters such as the rotational and traverse speeds of the tool on the microstructural and mechanical properties of copper plates were investigated; additionally, Charpy tests were performed on copper plates for the first time. Also, the effect of the number of welding passes on the aforementioned properties has not been investigated in previous studies. The results indicated that better welds with superior properties are produced when less heat is transferred to the workpiece during the welding process. It was also found that although the properties of the stir zone improved with an increasing number of weld passes, the properties of its weakest zone, the heat-affected zone, deteriorated.

Keywords: copper; friction stir welding; mechanical properties; microstructure

1. Introduction

The friction stir welding (FSW) method is a new method used to join materials; it is widely used in different industries, including the automobile and aerospace industries [1]. This method has several advantages compared to common welding methods. These advantages include nearly defect-free welds with minimal tiny cracks; the occurrence of the recrystallization phenomenon, resulting in finer crystallization compared to the initial material; and welds with minimal distortion [2]. Considering the fact that this type of welding is performed in the solid state, different pieces of materials can be joined, avoiding the problems of fusion welding [3]. This welding method was invented and introduced by The Welding Institute (TWI), Cambridge, United Kingdom in 1991 [4].

The FSW method can be used for various types of materials such as aluminum alloys [3], magnesium [5], copper, nickel alloys, steel, titanium [6], and many polymeric materials [7]. In this study, copper was chosen because along

with its alloys, it is being increasingly used as a structural material [6]. Copper is known to have high resistance to corrosion, and remarkable electrical and thermal conductivity. These features have led to a wider use of this metal in various industries such as the electronics and lighting industries [8–9]. Furthermore, copper is used to produce pipes and ducts in many industries [10]. Also, because of its high resistance to corrosion, copper is used in the production of water pipelines [11–12] and in supplying water to homes [13]; thus, 80% of water systems around the world today are made of copper [14]. This metal is used in solar cells because of its appropriate electrochemical properties [15] and is also widely used in heat exchangers because of its high thermal conductivity [15–16].

Using traditional welding methods to join copper pieces is difficult because of the high melting point and thermal diffusivity of copper. In fact, due to these two factors, welding copper requires much heat and thus much energy. Meanwhile, the welding speed is reduced. Therefore, the FSW method is recommended for use in joining pieces of this metal [17]. However, few studies to date have investi-

Corresponding author: Ali Alavi Nia E-mail: alavi495@basu.ac.ir

© University of Science and Technology Beijing and Springer-Verlag Berlin Heidelberg 2016

gated the FSW of copper [18].

Lee and Jung [18] welded copper plates with a thickness of 4 mm with a tool moving at a traverse speed of 61 mm/min and a rotational speed of 1250 r/min and investigated the mechanical and microstructural properties of the welded plates. They found that the tensile strength of the welded sample was 87% of the tensile strength of the base metal. Likewise, Shen *et al.* [19] joined copper plates with a thickness of 3 mm using a tool with a constant rotational speed of 600 r/min and traverse speeds of 25, 50, 100, 150, and 250 mm/min. They investigated the mechanical properties of the welds, including the hardness and tensile characteristics, as well as their microstructural properties. Also, Xie *et al.* [20] welded copper plates with a constant traveling traverse speed of 50 mm/min and rotational speeds of 400, 600, and 800 r/min. They determined and compared the values of yield strength and ultimate strength, as well as the percentage of elongation to fracture, hardness, and grain size of the stir zone for each of the welding conditions. Sun and Fujii [8] studied the effect of the force exerted on the workpiece by the tool at different traverse and rotational speeds; they explained the changes in the samples based on microstructure changes. Khodaverdizadeh *et al.* [21] investigated the effect of pin shapes on the mechanical properties of welded plates using the friction stir method. They found that the samples welded with square pins had better mechanical properties than the ones welded with circular pins. More recently, Xu *et al.* [22] studied the effect of rapid cooling by liquid dioxide on the microstructural and mechanical properties of copper plates. They realized that rapid cooling can cause shrinkage of the zone affected by temperature and also improves its mechanical properties.

In this study, the effects of rotational speed and traverse

speed of the tool on the mechanical and microstructural properties of copper were investigated simultaneously. Changing these speeds directly influences the rate of heat transferred to the workpiece, which in turn will change the properties of the resulting weld. Moreover, the effect of two passes of FSW on the mechanical and microstructural properties of copper plates was also investigated. Also, to examine the resulting copper welds more precisely, the Charpy test, which has been previously performed on steel [23] and aluminum [24] samples, was utilized in the present study.

2. Experimental

2.1. Welding pieces

To carry out the tests, copper samples with lengths of 135 mm and widths of 50 mm were cut perpendicular to the rolling direction from a large sheet with a thickness of 5 mm. The content of the constituent elements of copper used in this study based on quantitative tests is presented in Table 1. After cutting the samples, they were sanded and polished on their welding sides, whose length was 135 mm. The sanding and polishing were done so that the sheets would all fit together perfectly and avoid the trapping of air between them, which could reduce the quality of the welds. After smoothing the intended sections, the samples were placed together in a die for the welding process and were fixed towards each other by the die constraints. In addition to keeping the two workpieces fixed towards each other, the die constraints pushed them to the bottom of the die, where a copper plate is embedded. This copper plate at the bottom of the die is responsible for cooling the workpieces. As can be seen in Fig. 1, the water enters the die via a hose, and flows under the copper plate and into the slots, which are created under

Table 1. Weight percentage of constituent elements of copper used in the study

													wt%	
Cu	Ag	Be	Co	Cr	Si	Ni	Fe	Al	Mn	P	Sn	Pb	Zn	
Balance	Trace	<0.001	0.01	<0.002	<0.005	<0.005	0.01	Trace	0.01	0.02	<0.01	<0.01	<0.01	

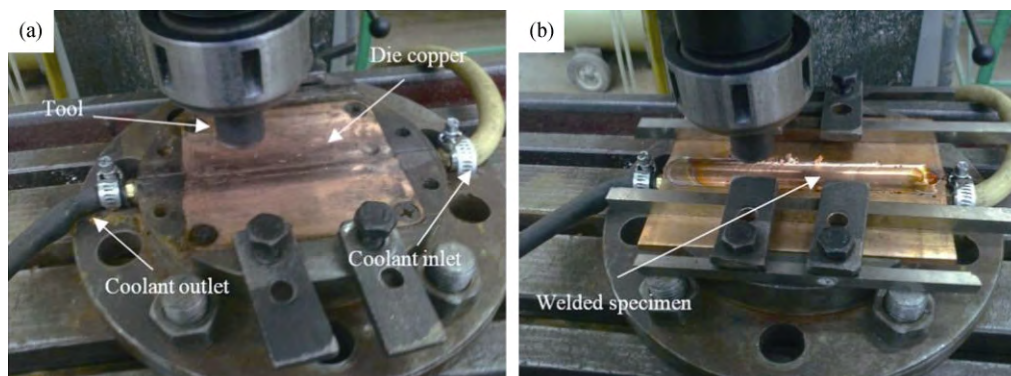


Fig. 1. View of (a) the tools and the die used in the welding process and (b) the pieces fixed to the die after the welding process.

the copper plate for this purpose; this has a cooling effect on the copper plate of the die. Also, the copper plate, which is in direct contact with the workpieces, serves to transfer heat from the workpiece to the water, thereby reducing the temperature of the workpieces.

After the cooling process, the water enters the outlet hose from the other side of the die and exits through it. The mass flow rate of water through the die is 0.019 kg/s. This type of cooling is performed to quickly transfer the heat from the workpieces, to prevent the grains in their microstructures from growing. In most previous studies, it has been acknowledged that cooling and rapid disposal of heat from pieces during the friction stir process will improve the properties of many materials [25–27].

The rotating tools used for the FSW process consist of a shoulder with a diameter of 20 mm and a pin with a diameter of 8 mm and a length of 4.7 mm. The pin contains a number of threads that permit the materials to move more smoothly around the tool and along its axis. Fig. 2 provides a view of this tool. The tool tilt angle is considered to be 2.5°. Also, the amount of shoulder plunging in the workpiece is 0.2 mm.

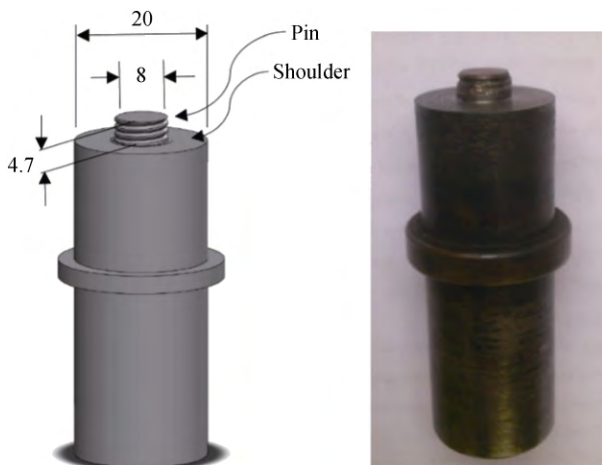


Fig. 2. Tool used for the FSW process (dimensions in mm).

The purpose of this study was to investigate the effects of different welding conditions in terms of the rotational speed and traverse speed of the tool, as well as the effects of the number of passes on the microstructural and mechanical properties of the welds. Therefore, the appropriate welding conditions for successful welding of the abovementioned samples were determined by welding under different conditions (presented in Table 2) and using a trial and error method. Images of the samples, which were produced through these different welding conditions, are given in Fig. 3.

Table 2. Different welding conditions used in the study

Case No.	Rotational speed / ($r \cdot \text{min}^{-1}$)	Traverse speed / ($\text{mm} \cdot \text{min}^{-1}$)
1	500	56
2	500	112
3	710	56
4 (2 passes)	500	56

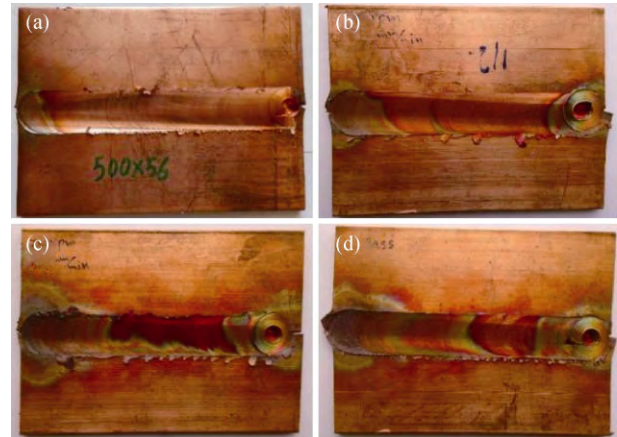


Fig. 3. Samples produced by different welding conditions: (a) in Case 1; (b) in Case 2; (c) in Case 3; (d) in Case 4.

After successful welding of the workpieces, a number of samples with appropriate dimensions were cut and separated for the hardness tests, and also their microstructures were observed. Then the workpieces were face milled from the top and also from the bottom by a milling machine before making tensile samples and Charpy tests' samples. The face milling from the top was performed so as to eliminate the excess edges created by the welding as well as the small dents, which were created on the surface by the penetration of the tool into the workpiece (0.2 mm). In addition, the face milling at the bottom of the workpiece was performed so as to eliminate the small seams remaining at the junction of the two workpieces and to prevent any effects on the results of the subsequent experiments. Due to the milling of these surfaces, the thickness of the workpieces was reduced from 5 mm to 3.7 mm.

It should be noted that the tensile tests, Charpy tests (impact toughness), hardness tests, and microstructure observations were conducted on the samples after the welding process.

2.2. Determining the weld zones and the grain sizes

In order to determine the different triple zones and examine their microstructures after welding, the samples were cut perpendicular to the welding line with a size slightly larger than the width of the welding line. The samples were

then sanded and polished well. Following the polishing process, the samples were etched using an appropriate etching solution. An appropriate solution for this purpose contains 10 g iron chloride, 30 mL hydrochloric acid, 60 mL ethanol, and 60 mL distilled water; the samples were placed in this solution for 20 s.

2.3. Hardness determination

After joining the pieces and cutting them perpendicularly to the weld line, the Vickers hardness of the samples was measured along the midline (see Fig. 4). To do this, a load of 300 g was imposed on each sample for 10 s, and thus the hardness profile was obtained perpendicular to the weld line. The reason for choosing this amount and duration of load is that we wished to obtain a clear and visible picture of the diamond-shaped trace, which remains from the hardness tester on the sample.

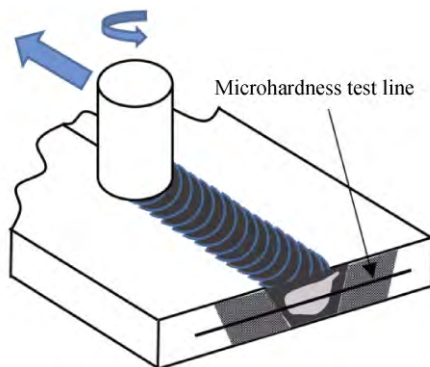


Fig. 4. Line of hardness testing (midline of the sample).

2.4. Tensile properties

In order to determine the tensile properties of the welded pieces, tensile tests were carried out perpendicular to the weld line according to the ASTM-E8 standard. The sizes of these samples were chosen so that all the different welding zones and a section of the base material of both sides of welding zones would be within the gauge length of the tensile samples. Fig. 5(a) shows the dimensions of the standard tensile samples. These samples were subjected to tensile tests using a 15-t Santam machine (Fig. 5(b)), and their stress-strain curves were obtained.

2.5. Impact toughness

In order to determine the impact toughness of the welded zone and compare it with the impact toughness of the base material, the specimens used in the Charpy impact test were prepared with the dimensions shown in Fig. 6. These specimens were prepared according to ASTM-E23-06 standards.

The specimens used for this test were small in size due to dimension limitations. All specimens were tested at ambient temperature using a device with a capacity of 15 J. In this experiment, the amount of absorbed energy because of fractures in the specimen was considered to be the impact toughness of the material. The Charpy test is in fact the experimental measurement of fracture toughness; the results of this test are mostly used for quality control, not for design purposes [28].

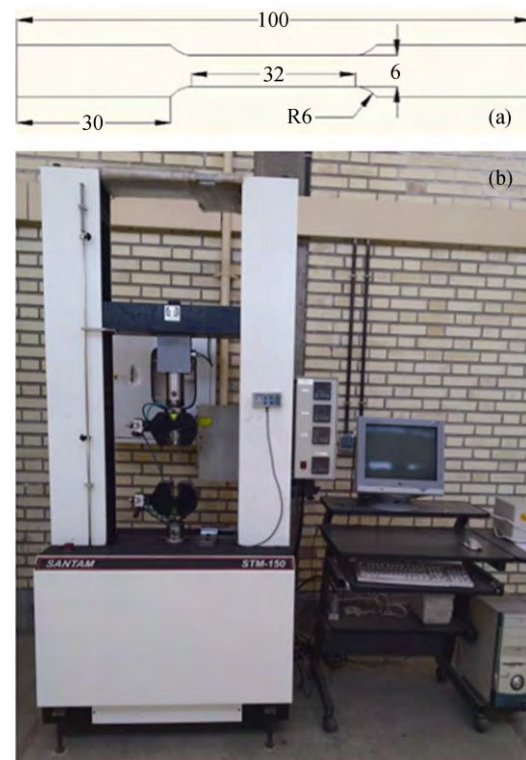


Fig. 5. (a) Dimensions of the standard sample for the tensile tests (mm) and (b) the Santam machine.

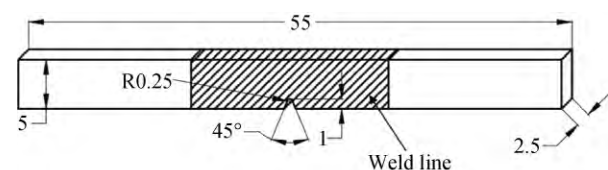


Fig. 6. Dimensions of Charpy test specimens (in mm).

3. Results and discussion

3.1. Weld zones and grain sizes

Although friction stir welding is performed in the solid state (without melting the material), the microstructure of the material undergoes significant changes. This process will change the properties of the material because of heat

being transferred to the workpiece and considerably deforming its shape [29]. These factors (heat and considerable deformation) create three different zones in the weld line. These zones include: (1) heat-affected zone, (2) thermo-mechanical-affected zone, and (3) stir zone. The stir zone is the area that undergoes overheating and thus considerable deformation, leading to dynamic recrystallization.

(a) Heat-affected zone (HAZ). This is two separate zones on both sides of the weld line, which undergo a thermal cycle during the welding process. This thermal cycle causes changes in the microstructure of this zone, which leads to changes in its mechanical properties, because the mechanical properties are dependent on the microstructure changes. The transfer of heat to this zone results in the creation of larger grains, which causes them to join either completely or partially. In other words, some grain boundaries are removed in this zone either completely or partially. It should be noted that no plastic deformation occurs in this zone.

(b) Thermo-mechanical-affected zone (TMAZ). Changes in this zone of the weld compared to the base material occur as a result of plastic deformations, which are caused by the tool and the heat caused by the welding process. This zone is divided into two areas: the area where recrystallization occurs and the area where recrystallization does not occur. The zone in which recrystallization does not occur is generally known as the thermo-mechanical-affected zone, while the other zone is called the stir zone. However, it should be noted that, generally, the thermo-mechanical-affected zone and the stir zone are defined as different and distinct zones in FSW joints. One feature of the thermo-mechanical-affected zone is the straining elongation of the grains as a result of mechanical forces and the expansion growth of the grains due to heat transfer.

(c) Stir zone (SZ). This is the section of the thermo-mechanical-affected zone, which has been recrystallized. This section is in fact the zone where the greatest amounts of deformation occur.

Fig. 7 shows a schematic presentation of the abovementioned zones and some technical terms used in friction stir welding. Other terms that it seems necessary to define are the advancing sides and retreating sides of the welds. In the stir friction process, the advancing side is a side of the workpiece (or tool) in which the direction of the rotational speed and traverse speed of the tool is the same, whereas the retreating side refers to the side where these two speeds have opposite directions [30].

After the etching process, the triple zones were determined for each of the welding conditions presented in Table

2 and Fig. 8. Furthermore, the crystallization of different zones was visible after etching the pieces. As an example, Fig. 9 displays the microstructure of the base material and the three welding zones in Case 1.

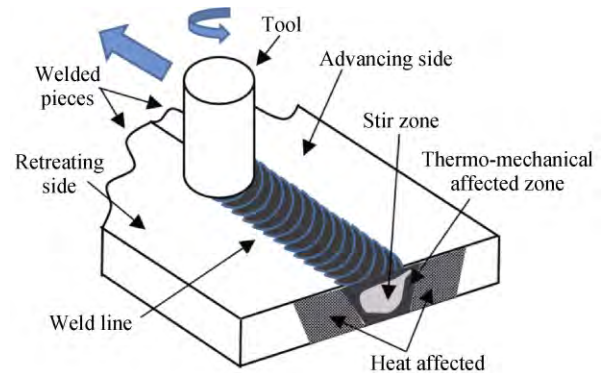


Fig. 7. Schematic of friction stir welding and its related expressions.

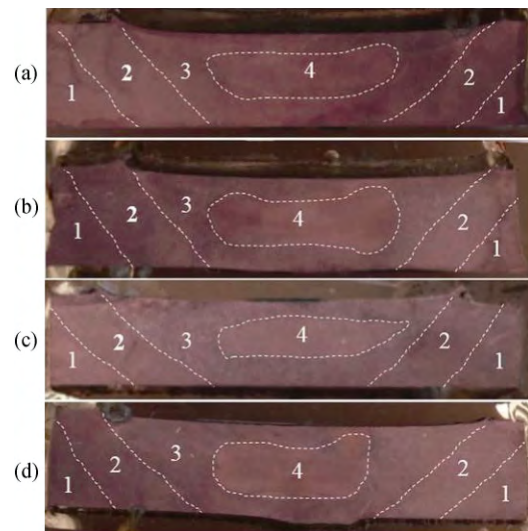


Fig. 8. Different zones created by welding under different welding conditions (1: base material; 2: heat-affected zone; 3: thermo-mechanical-affected zone; 4: stir zone): (a) in Case 1; (b) in Case 2; (c) in Case 3; (d) in Case 4.

Fig. 8 shows different zones resulting from the welding process under different welding conditions. As is clear from Figs. 8(a)-8(d), the stir zone is slightly inclined to the advancing side (i.e., the right side), which is because of the relatively higher speed of the advancing side in comparison to the retreating side. At a higher rotational speed (i.e., Case 3), specifically, the stir zone is generally moved slightly to the right side because of the higher speed of the advancing side in comparison to the retreating side. The microstructures of the different welding zones and the base material in Case 1 are shown in Fig. 9.

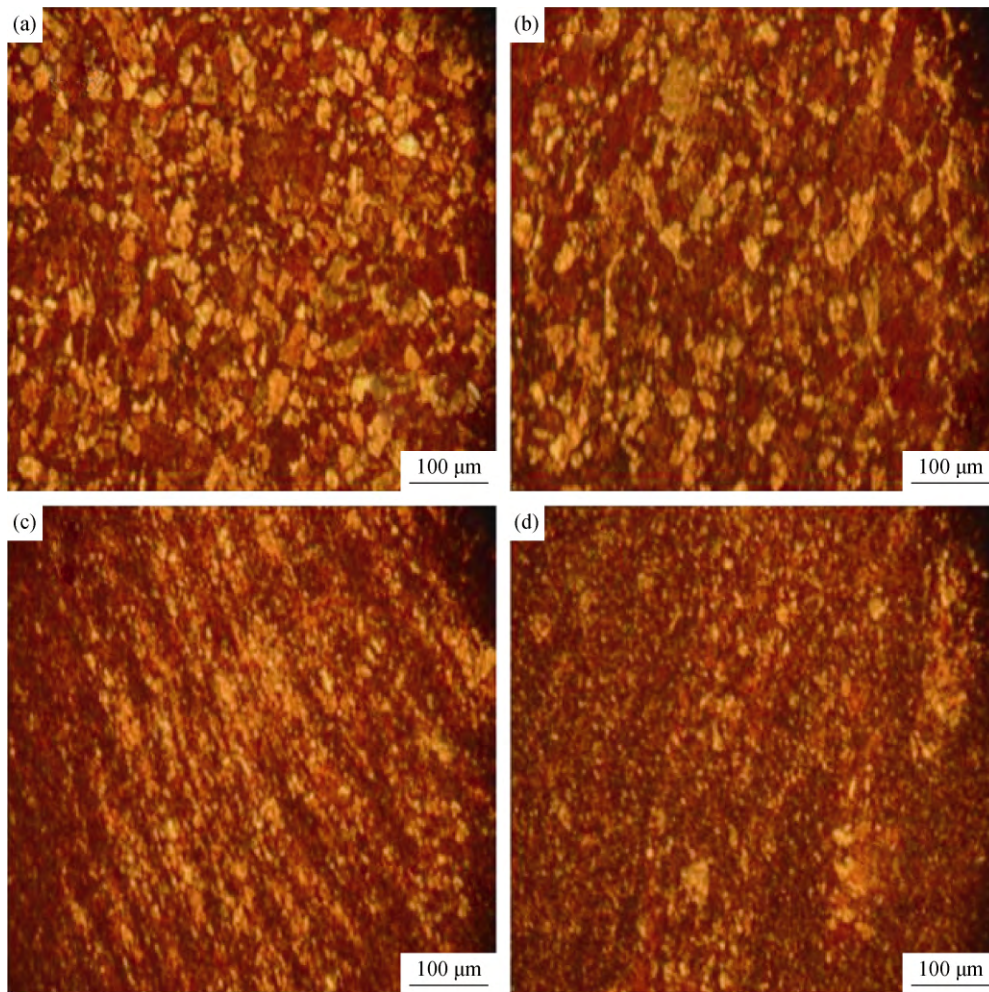


Fig. 9. Microstructures of the base material and the microstructure of the other zones created as a result of welding in Case 1: (a) base material; (b) heat-affected zone; (c) thermo-mechanical-affected zone; (d) stir zone.

Based on what is shown in Fig. 9, it can be observed that, due to recrystallization, the grain size in the stir zone is much smaller than that of the base material and the other zones mentioned earlier. The straining elongation of the grains is also clearly visible in the thermo-mechanical-affected zone. Creating this type of strain in this zone will lead to strain hardening, which improves mechanical properties such as hardness and strength. In contrast, the heat transferred to this zone will result in the creation of

slightly larger grains, leading to deterioration of the mechanical properties. Thus, this zone has properties similar to both the stir zone and the heat-affected zone, which in fact, can be considered as a transition zone. Fig. 9 also shows that the heat cycle has led to the creation of larger grains in the heat-affected zone. Hence, it is evident that the stir zone and heat-affected zone are more important, and have more crucial roles in determining the mechanical properties. Table 3 shows the grain size of these zones determined for all the

Table 3. Grain sizes and the amount of change in the heat-affected zone and the stir zone under different welding conditions

Case No.	Heat affected zone		Stir zone	
	Grain size / μm	Variation with respect to the base metal / %	Grain size / μm	Variation with respect to the base metal / %
1	20.1	16.2	4.2	-75.7
2	18.3	5.8	2.7	-84.4
3	23.4	35.3	13.5	-22.0
4	22.6	30.6	2.4	-86.1
Base metal (BM)	17.3	—	17.3	—

welding conditions through intersecting lines. The grain sizes obtained for the heat-affected and stir zones presented in Table 3 are justifiable because of the heat being transferred to the workpiece and considering the fact that an increase in the tool rotational speed will increase the heat transferred to the workpiece, while an increase in the traverse speed will decrease the heat transferred to the workpiece. A point which seems necessary to mention is that the grain size of the stir zone in Case 4 is smaller than that in Case 1; however, the grain size of the heat-affected zone under the same conditions is larger. It is obvious that the reason for the first phenomenon is that recrystallization has occurred twice in the stir zone and the reason for the second phenomenon is that the heat-affected zone has been affected by the two welding heat cycles.

3.2. Hardness

Fig. 10 shows the hardness profiles, which have been obtained for the different samples. As can be seen in Fig. 10, the hardness of the workpieces will be generally reduced by increasing the rate of the heat transferred to them during the welding process. Therefore, when the rotational speed is 710 r/min (i.e., Case 3), a great deal of heat is transferred to the workpiece; the lowest hardness can be seen in all three zones of this workpiece. In contrast, with a rotational speed of 500 r/min and a traverse speed of 112 mm/min (i.e., Case 2) in which less heat is transferred to the sample, the degree of hardness is relatively high. This is, in fact, justifiable according to the effect of the degree of heat transfer to the workpiece on its grain size. That is, when the transferred heat is greater, the size of the grains will increase, while the hardness will decrease. Also, considering Fig. 10, it can be seen that the highest degree of hardness in the stir zone is observed in Case 4, which is because of the reoccurrence of

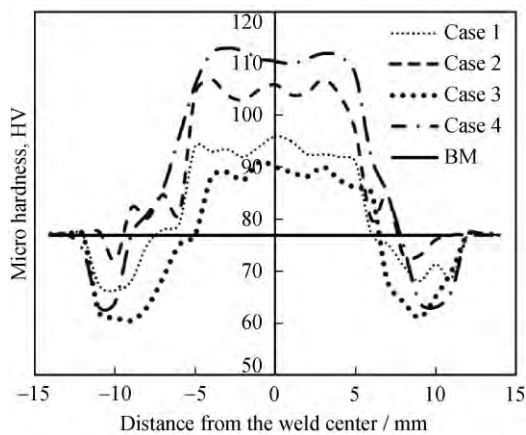


Fig. 10. Hardness profiles for the different welding conditions.

recrystallization and thus a considerable decrease in grain size.

3.3. Tensile properties

Fig. 11 shows the diagrams of true stress–logarithmic strain for the different welding conditions. Figs. 12(a)–12(d) also show the fractured samples after the tensile tests. Considering the results, it was found that all tensile test samples prepared from the welded pieces were fractured from the heat-affected zone. Other researchers in this field have also reported the same conclusion [17]. This confirms that the heat-affected zone is in fact the weakest welding zone in terms of tensile strength. The reason might be the large sizes of grains in this zone compared to other welding zones and the base material, which is because of the heat cycle during the welding process. As can be seen in the above section, this zone has also the lowest degree of hardness. Thus, it can be concluded that the heat-affected zone is the weakest welding zone.

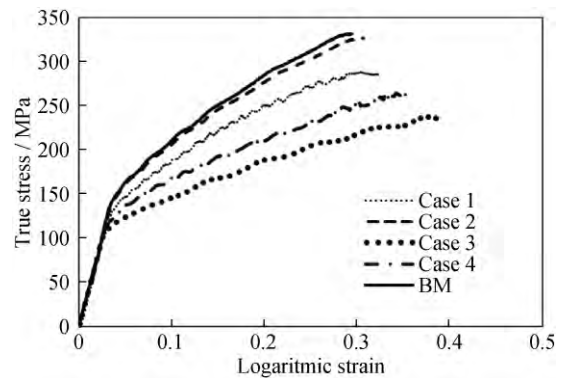


Fig. 11. Diagrams of true stress–logarithmic strain for different welding conditions.



Fig. 12. Tensile samples of different welding conditions: (a) Case 1; (b) Case 2; (c) Case 3; (d) Cases 4.

Sun and Fujii [6] added SiC particles to the area welded to copper as the base material during friction stir welding. They performed experiments with one and two welding

passes; they then examined the effects on the mechanical and microstructural properties of the obtained welds and compared the results with those from a one pass weld without added SiC particles. They found that in the two-pass weld, the heat-zone had lower hardness than in the one-pass weld; however, adding the particles increased the hardness in general. On the other hand, the tensile strength in the two-pass weld was higher than that in the one-pass weld with added particles. The tensile strength of the two-pass weld with added particles was approximately as high as the tensile strength of the two-pass weld without extra particles. That is, in general, the presence of these extra particles reduced the properties in terms of strength, and this reduction was less noticeable in the two-pass weld. They attributed this finding to a better distribution of SiC particles in the base material of the two-pass weld. However, the fracture point location in the tensile tests they conducted was different from what was observed in this study. In fact, the frac-

ture point in all the experiments they carried out was not observed in the heat-affected zone.

To facilitate the comparison of the tensile properties of the welds, the data displayed in Fig. 11 is presented in tabular form in Table 4. Table 4 indicates that the yield stress and ultimate stress of the base material are the highest among the samples, while its amount of strain to fracture is the lowest. This is because of the annealing of the heat-affected zone in the welded samples, which led to a decrease in tensile strength and an increase in fracture strain. Comparing the tensile results of the welded samples, we found that by increasing the amount of heat transferred to the workpieces during the welding process, the degree of annealing is increased as well. This shows the importance of cooling. Fig. 13 shows a schematic presentation of two joined sheets, the direction in which the tensile samples were extracted, and their fracture points (heat-affected zone).

Table 4. Tensile properties of the base material and welds under different welding conditions

Case No.	Yield strength / MPa	Variation with respect to the base metal / %	Tensile strength / MPa	Variation with respect to the base metal / %	Failure elongation	Variation with respect to the base metal / %
1	129	-5.8	284	-14.2	0.32	10.3
2	134	-2.2	326	-1.5	0.31	6.9
3	106	-22.6	235	-29.0	0.38	31.0
4	114	-16.8	263	-20.5	0.35	20.7
Base metal	137	—	331	—	0.29	—

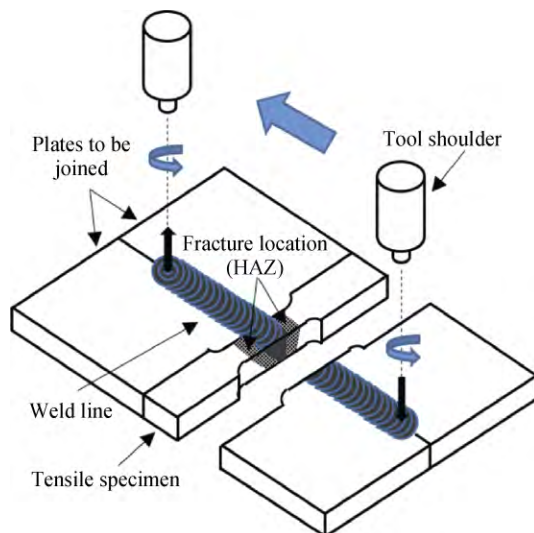


Fig. 13. Schematic presentation of two joined sheets, the direction in which the tensile samples were extracted, and their fracture points (heat-affected zone).

In addition to optical microscopic photos, scanning electron microscopic (SEM) images were used to characterize the microfracture surfaces of the tensile tested specimens to

understand the failure patterns. Fig. 14 shows a comparison of the tensile fracture features of the base metal, Case 2, and Case 3. All of the fractured surfaces consist of dimples of varying size, which indicates that all of the failures are the result of ductile fractures. Also, this figure shows that deep-hole type dimples are found in the Case 3 sample, while shallow-hole type dimples are observed in the fracture features of the base metal and the Case 2 sample. It can be seen that the dimple size in Case 2 is approximately the same as that of the base metal. Thus, it can be concluded that the sample welded under higher heat input conditions (Case 3) shows larger voids in its fracture surface and is weaker; however, the fracture surface of the sample welded under lower heat input conditions (Case 2) shows smaller voids, and its tensile strength is superior to that of the other welding conditions and closer to the tensile strength of the base metal.

It seems essential to note that the surface of contact between the two plates to be joined should be prepared so that they fit perfectly together; this prevents the trapping of air, which would weaken the weld. This is also the purpose of

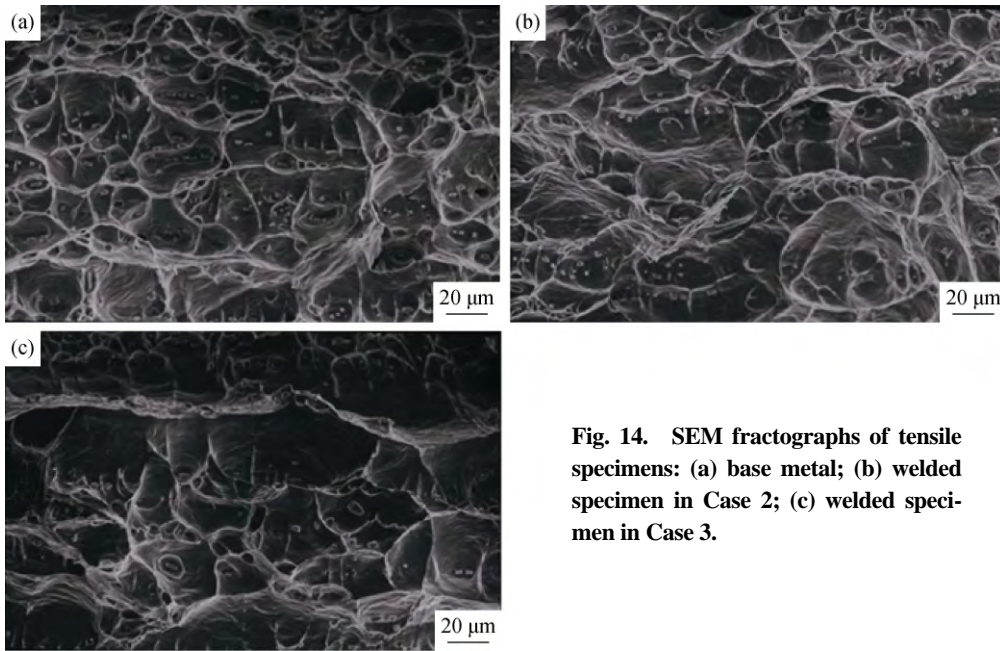


Fig. 14. SEM fractographs of tensile specimens: (a) base metal; (b) welded specimen in Case 2; (c) welded specimen in Case 3.

the initial sanding and polishing of the contact point of two pieces mentioned earlier. If air bubbles become trapped in the junction of the welds, their negative effect on the tensile properties of the samples cannot be eliminated even by increasing the number of welding passes. Figs. 15(a) and 15(b) shows the samples obtained under welding conditions of one and two passes (Case 1 and Case 4), which are weakened because of the presence of air. Also, Fig. 15(c) shows

the SEM image of a typical fracture surface of a weakened sample, and Fig. 15(d) indicates its gas holes, with 80-fold magnification. As can be seen in this figure, under both conditions, the weld is broken from the contact point of the two pieces and not from the heat-affected zone. It is clear that the amount of force required to fracture the samples under this condition is lower because the samples have less strength due to the presence of air.

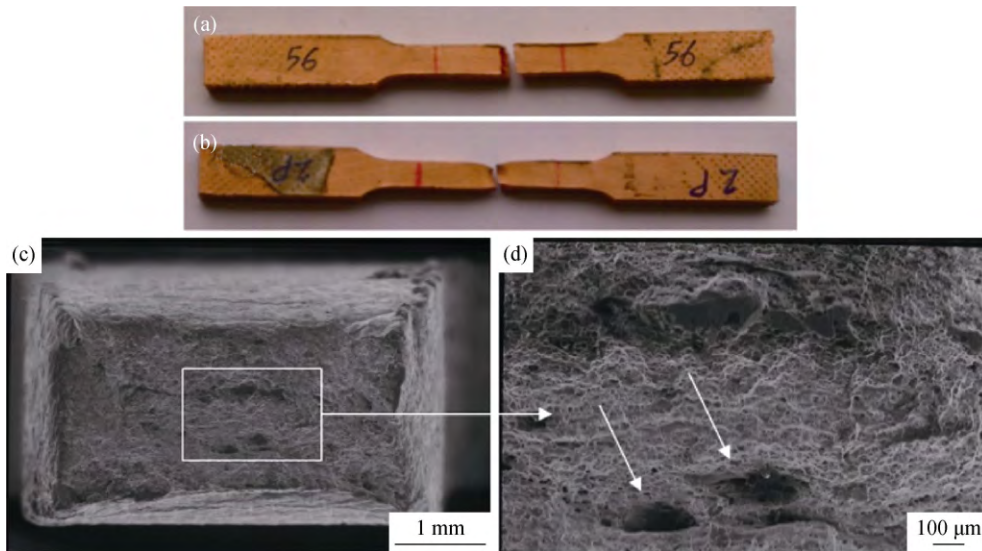


Fig. 15. Samples weakened because of air trapped in the welding point: (a) Case 1; (b) Case 4; (c) a typical fracture surface of a weakened sample; (d) gas holes in this fractured surface.

3.4. Impact toughness

Table 5 indicates the results of the Charpy test for the dif-

ferent welding conditions. Considering that the grooves of the Charpy test specimens are all located in the stir zone, we can infer from Table 5 that carrying out friction stir

welding in all cases led to an increase in the impact toughness. Particularly, in Case 4, this energy increased by about 81%. This energy increase is because of the fact that in Case 4, the size of the grains decreased dramatically because of the reoccurrence of recrystallization in the stir zone. In fact, the grain size was reduced up to 86.1% of that of the base material. Generally, as shown in Table 5, it can be inferred that the smaller the size of the grains, the greater the impact toughness. Figs. 16(a)–16(e) show the Charpy test specimens after fracture.

Table 5. Results obtained from Charpy test for different welding conditions

Case No.	Impact toughness / J	Increase with respect to the base metal / %
1	6.7	26.4
2	7.3	37.7
3	5.8	9.4
4	9.6	81.0
Base metal	5.3	—

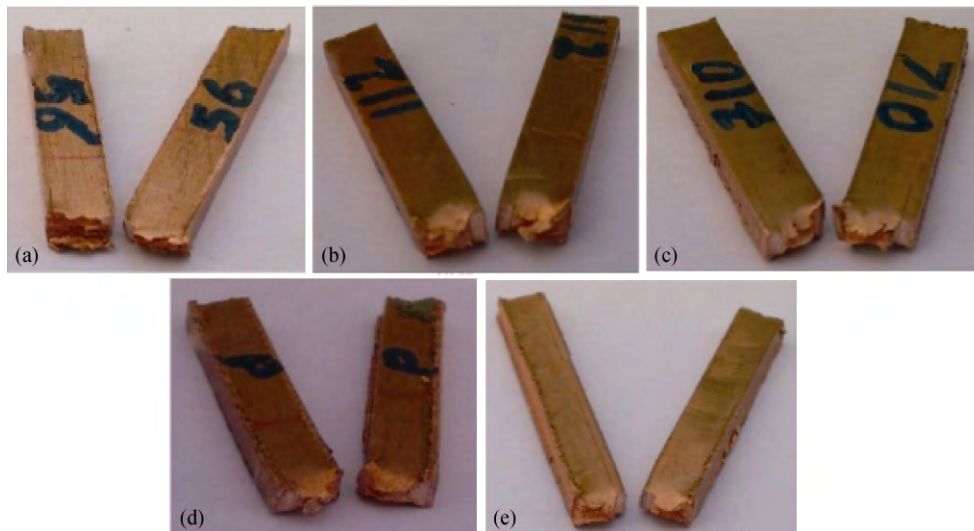


Fig. 16. Charpy test specimens after fracture for (a) Cases 1, (b) Case 2, (c) Case 3, (d) Case 4, and (e) the base material, respectively.

4. Conclusions

In this study, copper plates with thicknesses of 5 mm were joined using the FSW method with different traverse and rotational speeds of the tool for one or two passes. After the welding process, changes occurred in the mechanical properties, including the impact toughness and microstructure, and the relationship between the processes and the changes were investigated. The results of this study are summarized below:

(1) The conditions presented in Table 2, that is, combinations of rotational speeds of 500 and 700 r/min, and traverse speeds of 56 and 112 mm/min are appropriate conditions for performing successful and defect-free welding on copper samples.

(2) The samples should be aligned well on the surfaces where they are to be welded. They must be fitted together carefully so as to avoid trapped air that can weaken the tensile properties of the welds, as shown in this study.

(3) Various welding conditions such as different rotational and traverse speeds of the tool have a large effect on

the amount of heat transferred to the samples, which has a direct impact on the mechanical and microstructural properties of the samples. For example, in Case 3, the grain size in the heat-affected zone increased by about 35.3% compared to the grain size of the base material, whereas in Case 2, the grain size increased only by 5.8%. This issue caused the tensile strength in Case 3 to decrease by about 29%. However, in Case 2, the tensile strength decreased by only 1.5%.

(4) In all four welding conditions mentioned in this study, the weakest welding zone was found to be the heat-affected zone, which was weaker than the other zones in terms of hardness and tensile properties. For example, the yield strength in this zone at the rotational speed of 710 r/min was reduced by about 22.6%, and its tensile ultimate strength was reduced by 29% compared to the base material. This weakness can be accounted for by the enlargement of the grains in this zone, which can be lessened by increasing the traverse speed or decreasing the rotational speed of the tool, or by cooling.

(5) Although using a higher number of welding passes will improve the properties of the stir zone, it will cause more weaknesses in the heat-affected zone and will result in

deterioration of the total mechanical properties of the welds. Thus, it is recommended that, instead of increasing the number of passes to improve the welds, the welding process should be carried out at lower temperatures.

References

- [1] H. Lombard, D.G. Hattingh, A. Steuwer, and M.N. James, Effect of process parameters on the residual stresses in AA5083-H321 friction stir welds, *Mater. Sci. Eng. A*, 501(2009), p. 119.
- [2] W. Woo, H. Choo, D.W. Brown, Z. Feng, and P.K. Liaw, Angular distortion and through-thickness residual stress distribution in the friction-stir processed 6061-T6 aluminum alloy, *Mater. Sci. Eng. A*, 437(2006), p. 64.
- [3] A. Steuwer, M.J. Peel, and P.J. Withers, Dissimilar friction stir welds in AA5083-AA6082: The effect of process parameters on residual stress, *Mater. Sci. Eng. A*, 441(2006), p. 187.
- [4] H.L. Qin, H. Zhang, D.T. Sun, and Q.Y. Zhuang, Corrosion behavior of friction-stir-welding joints of 2A14-T6 aluminum alloy, *Int. J. Miner. Metall. Mater.*, 22(2015), No. 6, p. 627.
- [5] D. Wang, J. Shen, and L.Z. Wang, Effects of the types of overlap on the mechanical properties of FSSW welded AZ series magnesium alloy joints, *Int. J. Miner. Metall. Mater.*, 19(2012), No. 3, p. 231.
- [6] Y.F. Sun and H. Fujii, The effect of SiC particles on the microstructure and mechanical properties of friction stir welded pure copper joints, *Mater. Sci. Eng. A*, 528(2011), p. 5470.
- [7] A. Bagheri, T. Azdast, and A. Doniavi, An experimental study on mechanical properties of friction stir welded ABS sheets, *Mater. Des.*, 43(2013), p. 402.
- [8] Y.F. Sun and H. Fujii, Investigation of the welding parameter dependent microstructure and mechanical properties of friction stir welded pure copper, *Mater. Sci. Eng. A*, 527(2010), p. 6879.
- [9] K. Surekha and A. Els-Botes, Development of high strength, high conductivity copper by friction stir processing, *Mater. Des.*, 32(2011), p. 911.
- [10] H. Khodaverdizadeh, A. Mahmoudi, A. Heidarzadeh, and E. Nazari, Effect of friction stir welding (FSW) parameters on strain hardening behavior of pure copper joints, *Mater. Des.*, 35(2012), p. 330.
- [11] P. Shi, Q. Wang, Y. Xu, and W. Luo, Corrosion behavior of bulk nanocrystalline copper in ammonia solution, *Mater. Lett.*, 65(2011), p. 857.
- [12] X. Zhang, S.O. Pehkonen, N. Kocherginsky, and G.A. Ellis, Copper corrosion in mildly alkaline water with the disinfectant monochloramine, *Corros. Sci.*, 44(2002), p. 2507.
- [13] J.J. Shim and J.G. Kim, Copper corrosion in potable water distribution systems: influence of copper products on the corrosion behavior, *Mater. Lett.*, 58(2004), p. 2002.
- [14] N. Boulay and M. Edwards, Role of temperature, chlorine, and organic matter in copper corrosion by-product release in soft water, *Water Res.*, 35(2001), p. 683.
- [15] S.O. Pehkonen, A. Palit, and X. Zhang, Effect of Specific water quality parameters on copper corrosion, *Corrosion*, 58(2002), p. 156.
- [16] L.E.A. Berlouis, D.A. Mamman, and I.G. Azpuru, The electrochemical behaviour of copper in alkaline solutions containing fluoride, studied by in situ ellipsometry, *Surf. Sci.*, 408(1998), p. 173.
- [17] A.M. Alfantazi, T.M. Ahmed, and D. Tromans, Corrosion behavior of copper alloys in chloride media, *Mater. Des.*, 30(2009), p. 2425.
- [18] W.B. Lee and S.B. Jung, The joint properties of copper by friction stir welding, *Mater. Lett.*, 58(2004), p. 1041.
- [19] J.J. Shen, H.J. Liu, and F. Cui, Effect of welding speed on microstructure and mechanical properties of friction stir welded copper, *Mater. Des.*, 31(2010), p. 3937.
- [20] G.M. Xie, Z.Y. Ma, and L. Geng, Development of a fine-grained microstructure and the properties of a nugget zone in friction stir welded pure copper, *Scripta Mater.*, 57(2007), p. 73.
- [21] H. Khodaverdizadeh, A. Heidarzadeh, and T. Saeid, Effect of tool pin profile on microstructure and mechanical properties of friction stir welded pure copper joints, *Mater. Des.*, 45(2013), p. 265.
- [22] N. Xu, R. Ueji, Y. Morisada, and H. Fujii, Modification of mechanical properties of friction stir welded Cu joint by additional liquid CO₂ cooling, *Mater. Des.*, 56(2014), p. 20.
- [23] A.K. Lakshminarayanan, V. Balasubramanian, and M. Salahuddin, Microstructure, tensile and impact toughness properties of friction stir welded mild steel, *J. Iron Steel Res. Int.*, 17(2010), p. 68.
- [24] R.S. Mishra and Z.Y. Ma, Friction stir welding and processing, *Mater. Sci. Eng. R*, 50(2005), p. 1.
- [25] A. Alavi Nia, H. Omidvar, and S.H. Nourbakhsh, Effects of an overlapping multi-pass friction stir process and rapid cooling on the mechanical properties and microstructure of AZ31 magnesium alloy, *Mater. Des.*, 58(2014), p. 298.
- [26] Y. Zhao, Q. Wang, H. Chen, and K. Yan, Microstructure and mechanical properties of spray formed 7055 aluminum alloy by underwater friction stir welding, *Mater. Des.*, 56(2014), p. 725.
- [27] L.G. Vigh and I. Okura, Fatigue behaviour of friction stir welded aluminium bridge deck segment, *Mater. Des.*, 44(2013), p. 119.
- [28] R. Nandan, T. DebRoy, and H.K.D.H. Bhadeshia, Recent advances in friction-stir welding: process, weldment structure and properties, *Prog. Mater. Sci.*, 53(2008), p. 980.
- [29] A.S. Franchim, F.F. Fernandez, and D.N. Travessa, Microstructural aspects and mechanical properties of friction stir welded AA2024-T3 aluminium alloy sheet, *Mater. Des.*, 32(2011), p. 4684.
- [30] Y.H. Yau, A. Hussain, R.K. Lalwani, H.K. Chan, and N. Hakimi, Temperature distribution study during the friction stir welding process of Al2024-T3 aluminum alloy, *Int. J. Miner. Metall. Mater.*, 20(2013), No. 8, p. 779.